Title	Crystal structure of lipoate-protein ligase A from Escherichia coli : Determination of the lipoic acid-binding site
Author(s)	Fujiwara, Kazuko; Toma, Sachiko; Okamura, Kazuko et al.
Citation	Journal of Biological Chemistry. 2005, 280(39), p. 33645-33651
Version Type	VoR
URL	https://hdl.handle.net/11094/73652
rights	© the American Society for Biochemistry and Molecular Biology.
Note	

Crystal Structure of Lipoate-Protein Ligase A from *Escherichia coli*

DETERMINATION OF THE LIPOIC ACID-BINDING SITE*

Kazuko Fujiwara[‡1], **Sachiko Toma**[§], **Kazuko Okamura-Ikeda**[‡], **Yutaro Motokawa**[‡], **Atsushi Nakagawa**[¶], **and Hisaaki Taniguchi**[‡‖]

From the [‡]*Institute for Enzyme Research, the University of Tokushima, Tokushima 770-8503,* [§]*Graduate School of Pharmaceutical Science, Kumamoto University, Oe-honmachi, Kumamoto 862-0973,* [¶]*Institute for Protein Research, Osaka University, Yamada-oka, Suita, Osaka 565-0871, and* [‖]*Harima Institute at SPring-8, RIKEN, Mikazuki, Sayo, Hyogo 679-5148, Japan*

Lipoate-protein ligase A (LplA) catalyzes the formation of lipoyl-AMP from lipoate and ATP and then transfers the lipoyl moiety to a specific lysine residue on the acyltransferase subunit of α-ketoacid dehydrogenase complexes and on H-protein of the glycine cleavage system. The lypoyllysine arm plays a pivotal role in the complexes by shuttling the reaction intermediate and reducing equivalents between the active sites of the components of the complexes. We have determined the X-ray crystal structures of *Escherichia coli* LplA alone and in a complex with lipoic acid at 2.4 and 2.9 Å resolution, respectively. The structure of LplA consists of a large N-terminal domain and a small C-terminal domain. The structure identifies the substrate binding pocket at the interface between the two domains. Lipoic acid is bound in a hydrophobic cavity in the N-terminal domain through hydrophobic interactions and a weak hydrogen bond between carboxyl group of lipoic acid and the Ser-72 or Arg-140 residue of LplA. No large conformational change was observed in the main chain structure upon the binding of lipoic acid.

Lipoic acid is a prosthetic group of acyltransferase (E2) subunit of the pyruvate, α-ketoglutarate, and branched-chain α-ketoacid dehydrogenase complexes and of H-protein of the glycine cleavage system (1–4). It attaches to a specific lysine residue on the proteins via an amide linkage between the ε-amino group of the lysine residue and the carboxyl group of lipoic acid. In the reaction sequence of the complexes, the lypoyllysine arm shuttles the reaction intermediates and reducing equivalents between the active sites of the components of the complexes.

The attachment of lipoic acid to the proteins occurs by two-step reactions in which a lipoyl-AMP intermediate is formed from lipoic acid and ATP, and pyrophosphate is released in the initial activation reaction (Reaction 1).
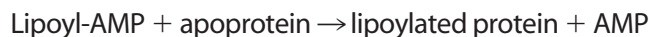
$$\text{Lipoate} + \text{ATP} \rightarrow \text{lipoyl-AMP} + \text{PP}_i$$

REACTION 1

The lipoyl moiety of the intermediate is then transferred to apoproteins in the second transfer reaction, yielding the lipoylated protein and AMP (Reaction 2).

$$\text{Lipoyl-AMP} + \text{apoprotein} \rightarrow \text{lipoylated protein} + \text{AMP}$$

REACTION 2

Lipoate-protein ligase A (LplA)[2] from *Escherichia coli* catalyzes the above two reactions. LplA activates and transfers not only naturally occurring R-(+)-lipoate but also S-(−)-lipoate, lipoate analogues, and octanoate to the apoproteins, although S-lipoate and octanoate are used at a 44 and 16% rate of R-lipoate, respectively (5, 6). LplA has a molecular mass of 37,795 Da, consisting of 337 amino acids excluding the initiating methionine residue, which is cleaved off during the biosynthesis (5). Strains with *lplA* null mutations have severe defects in the incorporation of exogenously supplied lipoic acid and lipoic acid analogues into apoproteins (5, 7).

In *E. coli*, there is another enzyme, LipB, responsible for the covalent attachment of lipoic acid. LipB transfers lipoic acid/octanoic acid endogenously synthesized on the acyl carrier protein by the function of LipA to the lipoate-dependent enzymes (7–9). LipB consists of 213 amino acids, whose amino acid sequence shares only 12.7% identity with that of LplA (Fig. 1). On the other hand, the amino acid sequence of LplA shows 31 and 35% identity with those of human and bovine lipoyltransferase, the mammalian LplA homologues, respectively (Fig. 1). However, the mammalian lipoyltransferases have no ability to activate lipoate to lipoyl-AMP and catalyze only the second half-reaction (10, 11). Strong homology in the N-terminal half region suggests that the region may be responsible for the second transfer reaction, whereas some residue(s) in the C-terminal region of the *E. coli* enzyme may be essential for the lipoate-activating reaction, which are lacking in the mammalian sequences (10).

To elucidate the structure-function relationship, we determined the crystal structure of LplA. We present here the structures of two forms of LplA: native and lipoate complex forms. LplA consists of two domains, the N-terminal and the C-terminal domains with a substrate binding pocket at the interface between these two domains. Lipoic acid is bound on the N-terminal domain side in the pocket through hydrophobic interactions. This is the first report on the crystal structure of the enzymes responsible for the lipoic acid metabolism.
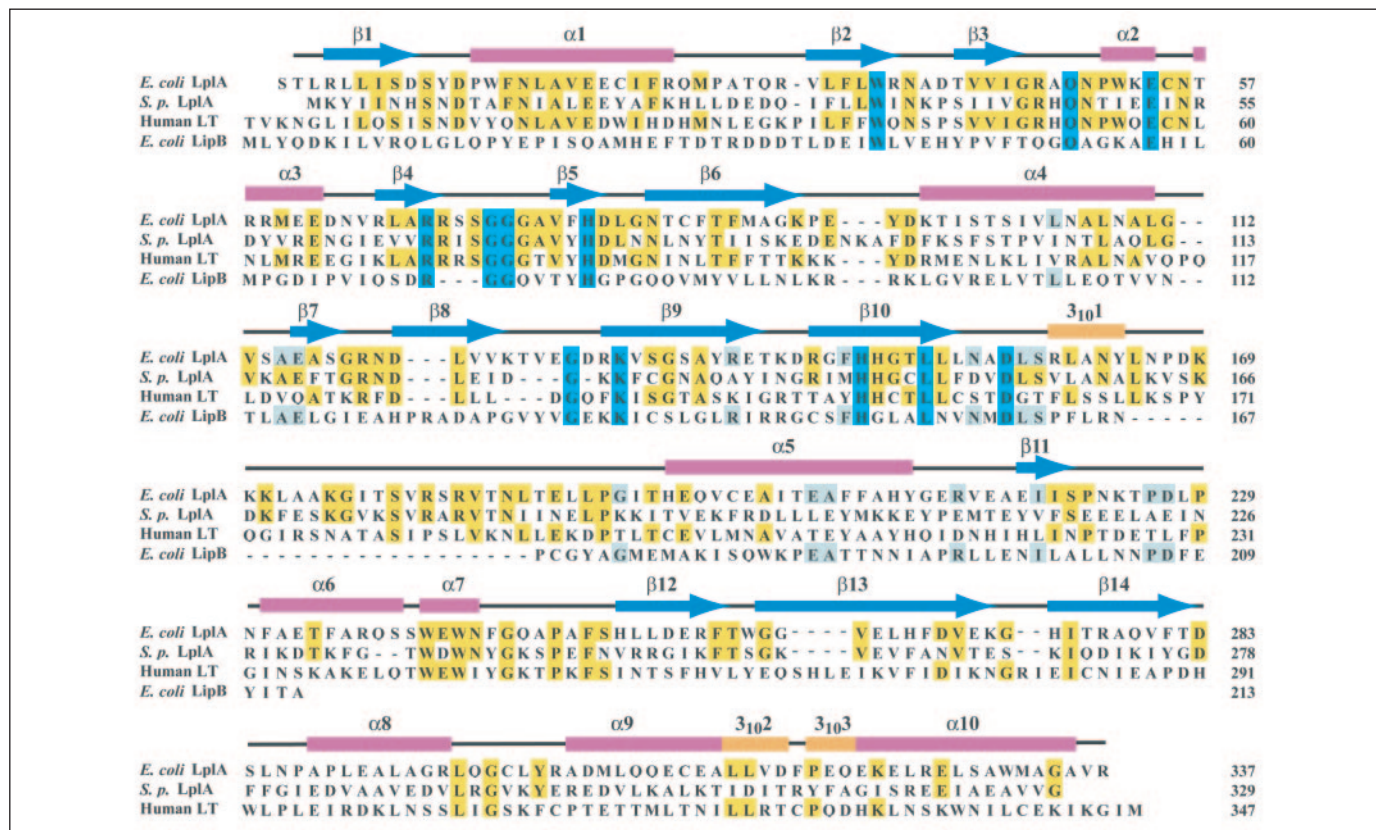
FIGURE 1. **The amino acid sequence alignment of *E. coli* and putative *S. pneumoniae* (*S. p.*) LplA, the human lipoyltransferase (*LT*), and *E. coli* LipB.** The residues conserved among four proteins, those between *E. coli* LplA and *S. pneumonia* LplA or human LT, and LipB are shown on a *blue*, *yellow*, and *green* background, respectively. The secondary structure elements of *E. coli* the LplA are assigned using the program DSSP (37). α-Helices, 3_{10}-helices, and β-strands are represented with *magenta rectangles*, *orange rectangles*, and *blue arrows*, respectively. Amino acid numbering of *E. coli* LplA starts at the serine residue following the initiation methionine residue (5), that of *S. pneumoniae* LplA starts at the initiation methionine residue (30), that of human LT starts at the N-terminal amino acid of the mature proteins (11), and that of LipB starts at the methionine residue added to the N-terminal extended active LipB (9). The sequence alignment was carried out using ClustalW (38).

EXPERIMENTAL PROCEDURES

Construction of the Expression Vector Containing lplA Gene—DNA manipulations were accomplished by the standard techniques (12). The gene encoding LplA was amplified by a PCR from the *E. coli* BL21(DE3) gene using a pair of oligonucleotides, 5′-AGGGTACCATATGTCCA-CATTACGCCTGCTCA-3′ (NdeI (underlined), Met (boldface letters), and nucleotides 86–104 (5)) and 5′-AGGGATCCCTACCTTACAGC-CCCCGCCAT-3′ (BamHI (underlined), Stop codon (boldface letters), and nucleotides 1096–1079) designed on the basis of the *lplA* sequence. The PCR product was inserted into the pET-3a expression vector (13). The construct pET-LPLA was verified by DNA sequencing and transformed into *E. coli* expression strain BL21(DE3)pLysS or B834(DE3)pLysS to obtain native LplA or selenomethionine-substituted LplA (Se-LplA), respectively. Cells were cultured in M9ZB (13) or Doublié and Carter medium supplemented with selenomethionine (30 mg/liter) (14) containing 25 μg/ml ampicillin, 25 μg/ml chloramphenicol, and 25 μM isopropyl-β-D-thiogalactopyranoside at 30 °C for 22 h. The bacterial cells were harvested by centrifugation.

Purification of the Recombinant LplA—Both LplA and Se-LplA were purified to homogeneity by the following method. *E. coli* cells were suspended in 40 mM Tris-HCl, pH 7. 5, 1 mM dithiothreitol (DTT), 40 μM (*p*-amidinophenyl) methanesulfonyl fluoride hydrochloride (APMSF), and 10 μg/ml leupeptin and lysed by sonication. The cell extract was obtained by centrifugation at 105,000 × *g* for 1 h and applied onto a hydroxylapatite column (3 × 6 cm) equilibrated with 3 mM potassium phosphate buffer, pH 7. 4. LplA was eluted with 4 mM potassium phosphate buffer, pH 7. 4, containing 0.5 mM DTT and 10 μM APMSF and further purified by a HiPrep 16/10 DEAE column (Amersham Bio-

sciences) equilibrated with 20 mM Tris-HCl, pH 7. 5, containing 0. 5 mM DTT and 10 μM APMSF. Proteins retained were eluted with a linear gradient of 0–0.2 M NaCl in the equilibration buffer. LplA fraction eluted at about 0. 1 M NaCl was concentrated with Centriplus YM-30 (Millipore Corp.) and applied onto a Superdex 200 pg 16/60 column (Amersham Biosciences). The column was developed with 40 mM Tris-HCl, pH 7.5, containing 1 mM DTT, 0. 5 mM EDTA, 10 μM APMSF, 5% glycerol, 0.16 M NaCl. In the Superdex gel, the protein behaved as a monomer.

Mutation of LplA—Mutations of S72A and R140A were introduced using an In-Fusion PCR Cloning kit (BD Biosciences Clontech). For the S72A mutation, PCRs were carried out employing pET-LPLA as a template and primer 1 (5′-AAGGAGATATACATATGTCCACAT-TACGC-3′ (pET-3a sequence (underlined) and then nucleotides 83–97 (5))) and primer 2 (5′- GCCACC**GGC**ACTGCGCCGCGCCAG-3′ (nucleotides 307–278; modified bases are shown in boldface letters)) to amplify the N-terminal half and primer 3 (5′- CGCAGT**GCC**GGTG-GCGGCGCGGT-3′ (nucleotides 293–326)) and primer 4 (5′-GTTAG-CAGCCGGATCCTAC-3′ (pET-3a sequence (underlined) and nucleotides 1099–1096)) to amplify the C-terminal half. For the R140A mutation, primer 1 and primer 5 (5′-GGTTTC**GGC**ATAGGC-CGAGCCTGAGA-3′ (nucleotides 511–486)) and primer 6 (5′-GC-CTAT**GCC**GAAACCAAAGATCGCGG-3′ (nucleotides 497–522)) and primer 4 were employed to amplify the N-terminal and C-terminal half, respectively. After the recombination reaction with pET-3a digested with NdeI and BamHI and the pair of the PCR products, the resultant plasmid was transformed into *E. coli* BL21(DE3)pLysS. The mutant LplAs were expressed and purified up to the DEAE-Sepharose

TABLE ONE

Data collection and refinement statistics

	Se-LplA	Se-LplA	Se-LplA·lipoate complex
Data collection			
Space group	$C222_1$	$C222_1$	$C222_1$
Cell dimensions (Å)			
a	81.6	82.0	83.2
b	112.1	112.8	111.6
c	289.2	289.4	289.6
Wavelength (Å)	0.9796	0.9000	0.9215
Resolution range (Å)	33.9–2.8	43.6–2.4	66.7–2.9
	$(3.0–2.8)^a$	(2.5–2.4)	(3.0–2.9)
No. of unique reflections	33,110	52,725	29,247
Completeness (%)	100 (99.9)	99.4 (99.7)	97.4 (99.0)
$I/\sigma (I)$	6.1 (1.0)	18.0 (2.9)	15.6 (3.8)
R_{merge} (%)^b	9.9 (66.6)	5.9 (29.7)	12.0 (42.1)
Structure refinement			
Resolution (Å)		43.6–2.4	66.7–2.9
No. of reflections		49,805	27,666
R^c/R_{free}^{d} (%)		17.1/23.3	18.6/27.1
r.m.s. deviation			
Bond length (Å)		0.021	0.020
Bond angle (degrees)		1.830	1.976
Atoms per asymmetric unit			
Protein		7895	7891
Lipoic acid			24
Water		530	22
Ramachandran plot			
Most favored (%)		89.9	85.7
Additional allowed (%)		9.7	14.0
Generously allowed (%)		0.3	0.2

^{a} The numbers in parentheses represent statistics in the highest resolution shell.
^{b} $R_{merge} = \Sigma\Sigma_j|\langle I(h)\rangle - I(h)_j|/\Sigma\Sigma_j\langle I(h)\rangle$, where $\langle I(h)\rangle$ is the mean intensity of symmetry-equivalent reflections.
^{c} $R = \Sigma\|F_o| - |F_c\|/\Sigma|F_o|$, where F_o and F_c are the observed and calculated structure factors for data used in refinement, respectively.
^{d} $R_{free} = \Sigma\|F_o| - |F_c\|/\Sigma|F_o|$ for 5% of the data not used at any stage of structural refinement.

step as described above. The purified wild-type and mutant LplAs in the DEAE-Sepharose fractions were apparently homogeneous on SDS-polyacrylamide gel electrophoresis and used for the steady state kinetic analysis.

Assay of LplA—The activity of LplA was determined in the reaction mixture of 50 μl containing 40 mM potassium phosphate buffer, pH 7.0, 0.3 mg/ml bovine serum albumin, 0.5 mM DTT, 3 μM *E. coli* apoH-protein as a lipoate acceptor, 30 μM R-(+)-lipoic acid, 2 mM ATP, 2 mM $MgCl_2$, and appropriate amounts of wild-type or mutant LplA. After preincubation for 90 s, the reaction was started by the addition of ATP or lipoic acid and carried out for 5 min at 37 °C. The reaction was terminated by heating the mixture at 95 °C for 70 s. The amount of lipoylated H-protein in the mixture was determined by the glycine-CO_2 exchange activity using *E. coli* P-protein as described previously (4). Apparent K_m values of wild-type and mutant LplA for lipoic acid, ATP, and apoH-protein were determined by varying the concentration of one substrate with a constant concentration of the other two substrates. The constant concentrations are the same as those in the standard assay mixture described above. The concentrations of varied substrates were 1.25–80 μM for lipoic acid, 2.5–1000 μM for ATP, and 0.188–4.5 μM for apoH-protein. R-(+)-lipoate was generously provided by ASTA-Medica (Frankfurt am Main, Germany). The recombinant *E. coli* apoH-protein was prepared as described for the preparation of holoH-protein

except that *E. coli* cells were grown in the medium without an addition of lipoic acid (15).

Crystallization—Crystallization was carried out at 20 °C by the hanging drop-vapor diffusion method using a protein solution dialyzed against 5 mM HEPES-Na, pH 7.5, and 3 mM DTT. Se-LplA was crystallized in a droplet containing a 1:1 ratio of protein solution at 3 mg/ml and reservoir solutions of 12.5–14.5% ethylene glycol and 21% glycerol. Crystals of Se-LplA·lipoate complex was grown with a modified protein solution at 5 mg/ml and a reservoir solution containing 3 mM R-(+)-lipoate.

Data Collection—All X-ray data were collected at 100 K on the beamline BL44XU at SPring-8 (Hyogo, Japan). The structure of Se-LplA was solved using Se-SAD methods (16). Before data collection, wavelength was calibrated by fluorescence scan of the Se-LplA crystal, and a wavelength was selected for data collection corresponding to the white line (peak, $\lambda = 0.9796$ Å). Data were collected in a 180° sweep in 1° oscillation steps, using an imaging plate detector, and then integrated and scaled with the programs MOSFLM (17) and SCALA (18). The data collection for crystal of Se-LplA·lipoate complex was carried out with a wavelength of 0.9215 Å sweeping 90° in 1° oscillation steps. The crystal containing lipoate was very weak against radiation damage; therefore, two data sets had to be merged to get enough data for the structure determination. Each data set was indexed and integrated with DENZO and then scaled and merged with SCALEPACK (19). The LplA crystals belong to space group $C222_1$ with unit cell dimensions of $a = 81.6$ Å, $b = 112.1$ Å, and $c = 289.2$ Å for Se-LplA crystal used for structure determination.

Structure Determination—All of the 15 expected selenium sites (for three monomers containing 5 Se-Met residues/asymmetric unit) were found using the heavy atom search program in CNS (20), and the initial phases were calculated with SHARP (21). 2.8 Å resolution maps calculated after density modification by SOLOMON (22) implemented in SHARP was used for determination of molecule mask and noncrystallographic symmetry operators for further density improvement. Solvent flattening, histogram mapping, and noncrystallographic symmetry averaging were applied for phase improvement using DM (23), and the resulting map was used for model building. The structure of Se-LplA·lipoate was solved by the molecular replacement method with MOLREP (24) in the CCP4 suite (25) using Se-LplA structure as a search model.

Model Building and Refinement—Model building and refinement for all structures were performed using the programs O (26) and REFMAC5 (27) in CCP4 suite (25), respectively. Refinement for Se-LplA was monitored with the R_{free} value calculated for a randomly selected 5% of reflections in the data set. The R_{free} values of Se-LplA·lipoate were calculated with the reflections, which were used for calculation of R_{free} values of Se-LplA. To build an Se-LplA structure, the quality of the initial experimental electron density map and known selenium sites allowed unambiguous tracing for the protein backbone and side chains. The protein model of Se-LplA was refined against the 43.6–2.4 Å resolution data set. The geometry library of lipoic acid was made using a monomer library sketcher in CCP4 suite (25). The Ramachandran plot was defined by PROCHECK (28).

RESULTS AND DISCUSSION

Structure Determination—Crystallization of *E. coli* LplA was mentioned about 10 years ago (6). The structure had never been determined, presumably because of the difficulty to obtain crystals suitable for the structural analysis. Hexagonal shape crystals of Se-LplA (0.06 × 0.08 × 0.1 mm) without substrate were obtained in 2 weeks by the hanging drop-vapor diffusion method, employing ethylene glycol as a precipi-

FIGURE 2. **The molecular architecture of LplA.** *A*, *ribbon* representation of three LplA molecules (MolA, MolB, and MolC) seen in the asymmetric unit in the *C*222₁ space group. MolA (*red*) and MolC (*blue*) are related by the noncrystallographic 2-fold symmetry. MolB (*green*) and MolB′ (*cyan*), which belongs to an adjacent asymmetric unit, are related by the crystallographic 2-fold symmetry. *Orange ellipses* show positions of the 2-fold axis. *B*, superposition of three crystallographically independent molecules (MolA (*red*), MolB (*green*), and MolC (*blue*)) in the asymmetric unit drawn by tube model of Cα trace. Although slight structural changes are found among these molecules (MolA-MolB, r.m.s. deviation 0.57 Å; MolA-MolC, r.m.s. deviation 0.70 Å; MolB-MolC, r.m.s. deviation 0.86 Å), overall fold shows almost identical structures except for some loop regions. *N* and *C* indicate the N and C termini, respectively. *C*, the stereo view of the native Se-LplA structure (MolC). The protein is shown as a *ribbon* representation with *blue* coloring at the N terminus along the *rainbow colors* to *red* at the C terminus. The lipoic acid molecule of MolA of the complex structure was superimposed and shown in a *ball-and-stick* mode. The figure was generated using MOLSCRIPT (39) and RASTER3D (40).
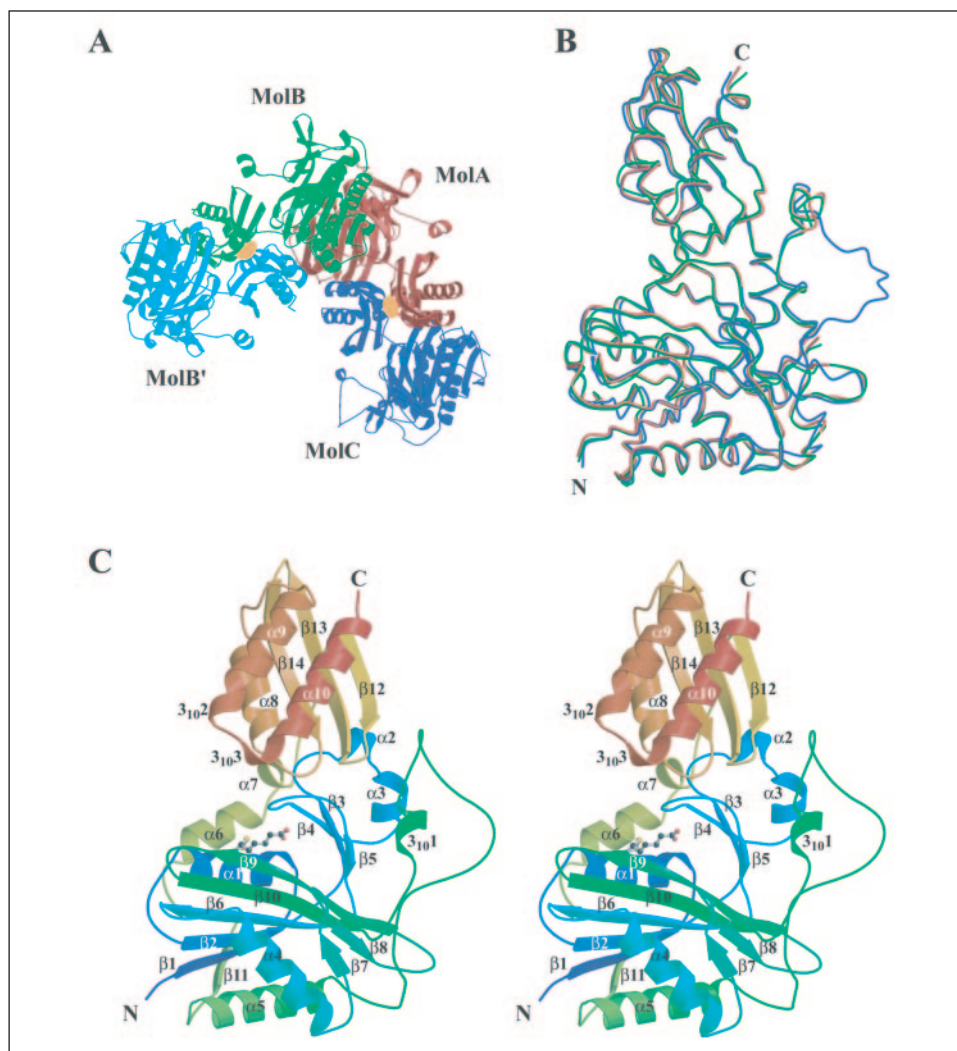
tant. The space group of the crystal was determined to be *C*222₁. The phase problem for LplA was solved by the SAD method, and the initial model could be built into the electron density. The final structure was refined using a 2.4 Å resolution data set, with cell dimensions of $a = 82.0$ Å, $b = 112.8$ Å, $c = 289.4$ Å. Results of the X-ray data collection and refinement statistics are summarized in TABLE ONE. Although cell dimensions were slightly changed among the crystals used, all crystals, the native and complex crystals, kept the same space group and similar cell dimension with a slight lack of isomorphism. There are three LplA molecules (MolA, MolB, and MolC) in the asymmetric unit (Fig. 2*A*). All residues (1–337) of the MolC could be assigned in the electron density; however, the density corresponding to residues 177–182 and 176–182 are missing in MolA and MolB, respectively. The final R factor for the reflection data used for refinement (working set) is 17.1%, and the R_{free} value is 23.3%. Superpositions of Cα positions of MolA and MolB, MolA and MolC, and MolB and MolC give root mean square (r.m.s.) deviations of 0.57, 0.70, and 0.86 Å, respectively. Despite relatively large r.m.s. deviations among the crystallographically independent molecules, they keep almost identical structures except for some loop regions (Fig. 2*B*). MolA and MolC are related by the noncrystallographic 2-fold symmetry, and they form a dimer structure. The same relationship is also found between MolB and the adjacent MolB related by a crystallographic 2-fold symmetry (MolB′). The contact surface area of MolA and MolC is 4507 Å² (13.6% of the sum of the surface area of the monomers), and that of MolB and MolB′ is 4196 Å² (12.9% of

surface area of the monomers) (29). Although the crystal structure of LplA shows dimer formation in a crystal, the gel filtration experiment shows that LplA is a monomer in solution. The dimer structure seems to be the result by the crystal packing.

Overall Structure of LplA Molecule—Fig. 2*C* shows a Cα trace of LplA (MolC). LplA consists of a large N-terminal domain (residues 1–244) and a small C-terminal domain (residues 253–337) connected by a single stretch of the polypeptide (residues 245–252). The N-terminal domain comprises two β-sheets, a large mixed β-sheet consisting of six strands (β₁, β₂, β₆, β₈, β₉, and β₁₀) and a small mixed β-sheet consisting of three strands (β₃–β₅), with seven α-helices (α₁–α₇) and a 3₁₀-helix (3₁₀1) surrounding the β-sheets. The C-terminal domain consists of three α-helices (α₈–α₁₀), two 3₁₀-helices (3₁₀2 and 3₁₀3), and a β-sheet comprising three strands (β₁₂–β₁₄). An open and solvent-exposed cleft is formed between the two domains. Fig. 1 shows the location of the secondary structure elements for the *E. coli* LplA, together with the amino acid sequence alignment of *E. coli* and putative *Streptococcus pneumoniae* LplA (30), human lipoyltransferase, and *E. coli* LipB. Amino acid residues well conserved among four proteins and between LplA and lipoyltransferase line inside of the cleft (on α₁, β₄ to β₅, β₉, and β₁₀). These results suggest that the cleft is a substrate-binding pocket.

The structure of LplA is similar to that of the putative lipoate-protein ligase from *S. pneumoniae* (Protein Data Bank accession code 1VQZ), which gives a Z-score of 29.8 for an alignment of 303/326 residue with an r.m.s. deviation of 3.1 Å and 31% sequence identity by the DALI
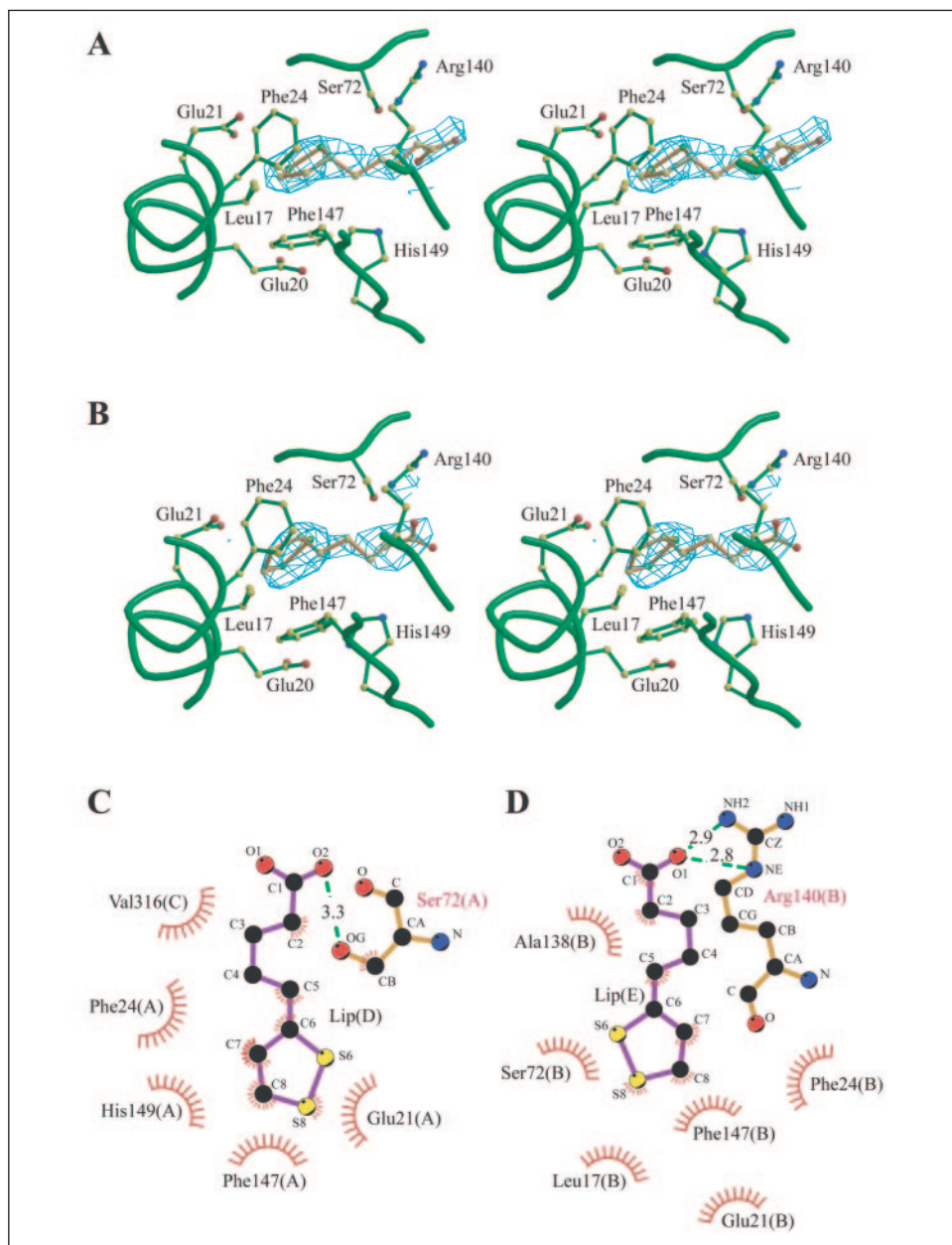
FIGURE 3. **The lipoic acid binding site.** Stereo views of the lipoic acid binding site in MolA (*A*) and MolB (*B*). The electron density of lipoic acid calculated with coefficients of the form σ_A-weighted $2mF_o - DF_c$ is plotted at the 1.0 σ level (*light blue*), where F_o is the native structure factor amplitude, and F_c is the calculated structure factor amplitude (25). Peptide chains of LplA are shown in *coil* representation (*dark green*). Amino acid side chains (*dark green*) and lipoic acid (*orange*) are shown in *ball-and-stick* mode. The figures were produced with BOBSCRIPT (41) and RASTER3D (40). *C* and *D*, schematic diagram showing the lipoic acid and LplA interactions in MolA and MolB, respectively. Lipoic acid and all of the LplA residues that interact with lipoic acid are shown in a *flattened* representation. Lipoic acid atoms with *short red lines* represent hydrophobic interactions pointing toward the LplA residues also outlined with *red lines*. The *green dashed lines* show potential hydrogen bonds between atoms with distance (in Å). This figure was generated with LIGPLOT (42).

program (31). The high structural similarity confirmed by superposition of the α-carbon traces of the putative protein and LplA suggests that the putative protein is a homologue of the *E. coli* lipoate-protein ligase A.

The Lipoic Acid Binding Site—Because lipoic acid is a labile compound, LplA crystals complexed with *R*-(+)-lipoic acid were obtained by seeding small crystals of the Se-LplA·lipoate complex into a droplet to accelerate the crystallization. Crystals suitable for analysis were obtained within 3 days after setting the droplet. The lipoic acid-bound form was determined at 66.7–2.9 Å resolution. Weak but significant electron density corresponding to lipoic acid was found in MolA and MolB (Fig. 3, *A* and *B*). Positions of the lipoic acid in MolA and MolB are slightly different. This may be caused by weak interactions between LplA and lipoic acid or insufficient information from low resolution data. Lipoic acid is located in a hydrophobic core generated by Leu-17, Phe-24, Phe-147, Ala-138, and aliphatic parts of Glu-21 and Ser-72 side chains. Hydrophobic interactions are formed between these residues and the dithiolane ring and the hydrophobic tail of lipoic acid. Leu-17, Ser-72, and Ala-138 are well conserved among LplAs and lipoyltrans-

ferase (Fig. 1). The electron density for the carboxyl group is weak relative to that for the hydrophobic moiety. In MolA, the carboxyl group makes a hydrogen bond with the side chain of Ser-72, whereas in MolB, the carboxyl group hydrogen bonds to the side chain of Arg-140 (Fig. 3, *C* and *D*). Although the actual binding mode may change somewhat when higher resolution x-ray data are eventually obtained, this complex provides insights into lipoic acid binding to the LplA molecule. Because van der Waals interactions are neither strong nor specific, and a weak hydrogen bond occurs only at the carboxyl group, it may permit LplA to bind not only *R*-(+)-lipoic acid but also *S*-(−)-lipoic acid, lipoic acid analogues, and octanoic acid. The binding mode well explains why LplA activates these carboxylic acids and transfers them to apoproteins (6, 7, 32). The reaction rates may be influenced by the slight differences in the van der Waals interactions between LplA and these substrates.

Functional and Structural Similarities to Other Proteins—A systematic analysis using the DALI program (31) identified a number of proteins/domains with significant structural similarities to LplA. The closest of them other than the LplA homologue is BirA, biotin holoenzyme

synthetase/bio repressor from *E. coli* (Protein Data Bank accession codes 1BIA and 1BIB) (33), which gives a Z-score of 9.4 for an alignment of 139/292 residues with an r.m.s. deviation of 3.5 Å and 12% sequence identity. BirA consists of three domains and functions as a repressor of the biotin biosynthetic operon and as an enzyme that catalyzes the activation and transfer of biotin to a specific lysine residue on the biotin-dependent carboxylases. The reaction mechanism is remarkably similar to that of LplA. The central domain contributes to the catalysis. Fig. 4
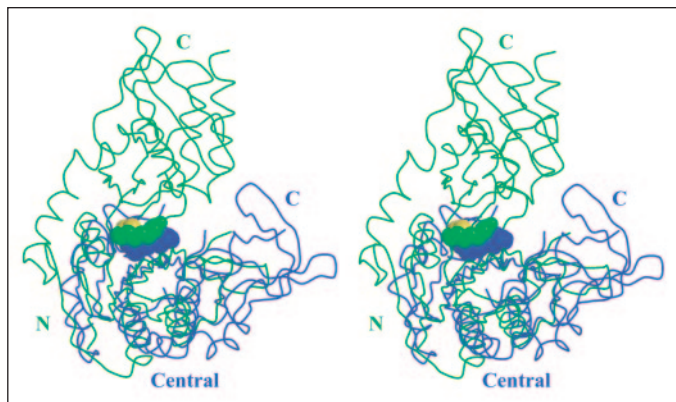

FIGURE 4. **Stereo view of the superimposed structure of LplA and BirA.** α-Carbon traces of LplA (*green*, MolA, residues 1–337) and BirA (*blue*, residues 68–317) are superimposed according to the matrices presented by DALI. The crystallographically observed lipoic acid (*green*) and biotin (*blue*) are shown in a *space-filling* representation. *N*, *Central*, and *C* indicate the N-terminal, central, and C-terminal domains of the respective *colored* protein. This figure was generated using MOLSCRIPT (39) and RASTER3D (40).

TABLE TWO

Kinetic constants for wild-type and mutant LplAs

Varied substrate	$K_{m(app)}$ [a]	$V_{max(app)}$ [a,b]
	μM	nmol/min/mg protein
Wild-type		
R-(+)-lipoic acid	4.5	219
ATP	15.8	133
ApoH-protein	1.2	258
S72A		
R-(+)-lipoic acid	8.9	178
ATP	295	160
ApoH-protein	1.1	212
R140A		
R-(+)-lipoic acid	0.55	6.0
ATP	13.7	8.4
ApoH-protein	15.5	28.1

[a] The values are presented as a mean of two or three separate experiments with an S.E. of less than 10%.

[b] Since an inhibition of the glycine-CO_2 exchange reaction was observed by the use of over 5 μM apoH-protein in the assay of LplA, a fixed concentration of 3 μM apoH-protein was used. Consequently, $V_{max(app)}$ values were underestimated when the concentrations of ATP and lipoic acid were varied.
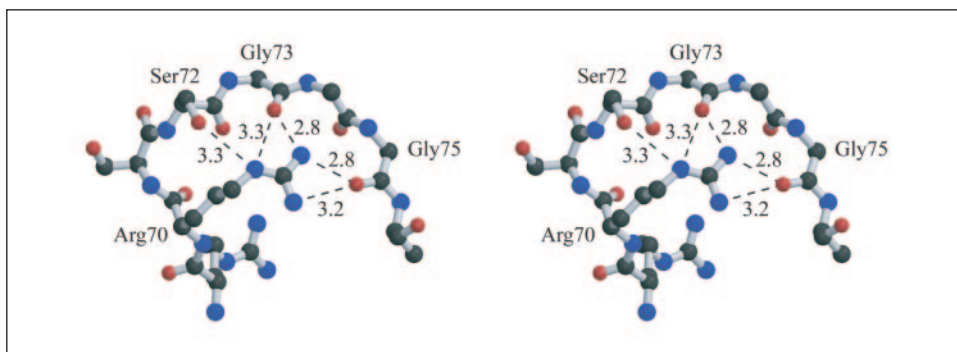
shows a superposition of LplA (residues 1–337) onto BirA (the central and C-terminal domains, residues 68–317) according to the rotation and translation matrices provided by DALI. Several α-helices (α_1, α_4, and α_5) and β-strands (β_1, β_2, β_6, β_7, β_9, and β_{10}) of LplA are well superimposed on the corresponding secondary structure elements of BirA. In both enzymes, lipoic acid and biotin interact with β-strands in the N-terminal domain and the central domain, respectively, and the substrates are situated in the similar position in the respective enzymes. Functional and structural similarities of these enzymes suggest that evolutionarily they are closely related, although they share only 12% amino acid sequence identity. The absence of a DNA binding domain in the LplA structure may be related to the finding that LplA metabolizes lipoic acid that is exogenously supplied rather than that synthesized endogenously in *E. coli* (5, 7).

Mechanistic Implication—Ser-72 and Arg-140 residues, respectively, were substituted by Ala to analyze the contribution of the residues to the lipoic acid binding (Fig. 3). Steady state kinetic studies were carried out by varying the concentration of one substrate and keeping the concentration of the other two substrates constant. Apparent kinetic constants are shown in TABLE TWO.

Whereas the S72A mutation results in an about 2-fold increase in $K_{m(app)}$ for lipoic acid, $K_{m(app)}$ for ATP is greatly increased by the mutation, indicating the reduced binding affinity for ATP. This result suggests that the hydrogen bond between lipoic acid and Ser-72 may not be so critical to fix lipoic acid at the position determined by the crystal structural analysis. However, the fixation of the carboxyl group to Ser-72 is required for the initiation of the lipoate activation reaction with ATP, or ATP may interact directly with Ser-72.

The R140A mutation results in reduced $V_{max(app)}$ values, although the values differ depending on the varied substrate because of the usage of the limited concentration of apoH-protein. $K_{m(app)}$ for lipoic acid is rather decreased. On the other hand, $K_{m(app)}$ for apoH-protein increases by 1 order of magnitude, indicating a reduction of the binding affinity for apoH-protein. In the protein lipoylation reaction, the presence of the Glu residue at the three residues N-terminal side from the Lys residue to be lipoylated in the lipoate acceptor protein is essential (34, 35). Therefore, Arg-140 in LplA may make a salt bridge with the Glu residue in the apoH-protein in the second transfer reaction (Reaction 2). These results of the kinetic analyses support the lipoic acid binding mode shown in Fig. 3 (*i.e.* lipoic acid is bound at the position by the hydrophobic interactions, and the weak hydrogen bond between the carboxyl group and the Ser-72 or the Arg-140 residue is enough to accommodate lipoic acid).

We attempted to obtain a crystal of the LplA·ATP complex by soaking the native crystal with Mg-ATP and by co-crystallization in the presence of Mg-ATP. However, X-ray analysis of the crystals did not show electron density for ATP clear enough to determine the ATP binding site. The first step of the reaction catalyzed by LplA is thought to

FIGURE 5. **The hydrogen bond network around Arg-70.** *Dashed lines* show potential hydrogen bonds between atoms with distances (in Å), which are the averaged values of three crystallographically independent molecules. This figure was generated with MOLSCRIPT (39) and RASTER3D (40).

be the nucleophilic attack of the carboxyl oxygen of lipoic acid on the α-phosphorus atom of ATP followed by the release of the pyrophosphate and the formation of a lipoyl-AMP intermediate by analogy to the reaction catalyzed by histidyl-tRNA synthetase (36). The activated carbon atom of the lipoyl-AMP intermediate is then attacked by the nonprotonated ϵ-amino group of the lysine residue of an apoprotein to be lipoylated, producing AMP and the lipoylated protein. To initiate the first reaction, ATP should be anchored near the lipoic acid in LplA, and especially the distance between the α-phosphorus atom of ATP and the carboxyl oxygen atom of lipoic acid should be less than 3 Å.

LplA has a characteristic sequence motif RRSSGGG between positions 69 and 75, which is highly conserved among the proteins listed in Fig. 1. The motif is situated on the loop following the β_4-strand (Fig. 2*C*) close to the bound lipoic acid. In the native LplA structure, the side chain of Arg-70 forms a hydrogen bond network with the main-chain carbonyl groups of Gly-73 and Gly-75 and the side chain of Ser-72, stabilizing the loop structure (Fig. 5). The motif can provide positive charges and a space large enough to accommodate ATP. Therefore, the motif is presumed to be involved in the binding of ATP or the adenylate moiety of the lipoyl-AMP intermediate. Indeed, the mutation of Ser-72 affects the binding affinity for ATP (TABLE TWO). An R72G point mutation in the human lipoyltransferase has been found in a hyperglycinemia patient, but no mutation has been found in the four proteins, P-, T-, L-, and H-protein, constituting the human glycine cleavage system.[3] The Arg-72 in the human lipoyltransferase corresponds to Arg-69 in *E. coli* LplA. The mutation may cause the reduction of the lipoylation level of H-protein of the glycine cleavage system, resulting in a decrease in the activity of the glycine cleavage system. The expression of the recombinant R72G mutant in *E. coli* failed presumably because of the instability of the mutant protein.[4] These findings also suggest that the motif plays an important role for the binding of the substrate or the stabilization of the three-dimensional structure.

Conclusions—The present study presents the LplA structure and its substrate binding site for the first time. LplA consists of a large N-terminal domain and a small C-terminal domain, comprising a substrate binding pocket at the interface of the two domains. Lipoic acid is bound to the N-terminal domain via hydrophobic interactions and a weak hydrogen bond to Ser-72 or Arg-140 in the pocket. The result well explains the reason why LplA utilizes lipoate analogues and octanoic acid in addition to the natural substrate, *R*-(+)-lipoate. The large solvent-exposed active site cleft is favorable to allow docking of the lipoate acceptor protein to initiate the second transfer reaction. In an effort to more fully define the active site geometry and to understand the reaction mechanism of LplA, co-crystallization studies of LplA with ATP and lipoyl-AMP are in progress.

REFERENCES

1. Reed, L. J., and Hackert, M. L. (1990) *J. Biol. Chem.* **265,** 8971–8974
2. Perham, R. N. (1991) *Biochemistry* **30,** 8501–8512
3. Fujiwara, K., Okamura-Ikeda, K., and Motokawa, Y. (1986) *J. Biol. Chem.* **261,** 8836–8841
4. Fujiwara, K., Okamura-Ikeda, K., and Motokawa, Y. (1992) *J. Biol. Chem.* **267,** 20011–20016
5. Morris, T. W., Reed, K. E., and Cronan, J. E., Jr. (1994) *J. Biol. Chem.* **269,** 16091–16100
6. Green, D. E., Morris, T. W., Green, J., Cronan, J. E., Jr., and Guest, J. R. (1995) *Biochem. J.* **309,** 853–862
7. Morris, T. W., Reed, K. E., and Cronan, J. E., Jr. (1995) *J. Bacteriol.* **177,** 1–10
8. Jordan, S. W., and Cronan, J. E., Jr. (1997) *J. Biol. Chem.* **272,** 17903–17906
9. Jordan, S. W., and Cronan, J. E., Jr. (2003) *J. Bacteriol.* **185,** 1582–1589
10. Fujiwara, K., Okamura-Ikeda, K., and Motokawa, Y. (1997) *J. Biol. Chem.* **272,** 31974–31978
11. Fujiwara, K., Suzuki, M., Okumachi, Y., Okamura-Ikeda, K., Fujiwara, T., Takahashi, E., and Motokawa, Y. (1999) *Eur. J. Biochem.* **260,** 761–767
12. Sambrook, J., Fritsch, E. F., and Maniatis, T. (1989) *Molecular Cloning: A Laboratory Manual*, 2nd Ed., Cold Spring Harbor Laboratory, Cold Spring Harbor, NY
13. Studier, F. W., Rosenberg, A. H., Dunn, J. J., and Dubendorff, J. W. (1990) *Methods Enzymol.* **185,** 60–89
14. Doublié, S., and Carter C. W., Jr. (1992) in *Crystallization of Nucleic Acids and Proteins* (Ducruix, A., and Giege, R., eds) pp. 311–317, Oxford University Press, New York
15. Okamura-Ikeda, K., Fujiwara, K., and Motokawa, Y. (1999) *J. Biol. Chem.* **274,** 17471–17477
16. Dauter, Z., Dauter, M., and Dodson, E. (2002) *Acta Crystallogr. Sect. D* **58,** 494–506
17. Leslie, A. G. W. (1999) *Acta Crystallogr. Sect. D* **55,** 1696–1702
18. Evans, P. R. (1993) in *Data Collection and Processing: Proceedings of the CCP4 Study Weekend* (Sawyer, L., Isaacs, N., and Bailey, S., eds) pp. 114–122, SERC Daresbury Laboratory, Warrington, UK
19. Otwinowski, Z., and Minor, W. (1997) *Methods Enzymol.* **276,** 307–326
20. Brünger, A. T., Adams, P. D., Clore, G. M., DeLano, W. L., Gros, P., Grosse-Kunstleve, R. W., Jiang, J.-S., Kuszewski, J., Nilges, M., Pannu, N. S., Read, R. J., Rice, L. M., Simonson, T., and Warren, G. L. (1998) *Acta Crystallogr. Sect. D* **54,** 905–921
21. de La Fortelle, E., and Bricogne, G. (1997) *Methods Enzymol.* **276,** 472–494
22. Abrahams, J. P., and Leslie, A. G. W. (1996) *Acta Crystallogr. Sect. D* **52,** 30–42
23. Cowtan, K. (1994) *Joint CCP4 and ESF-EACBM Newsletter on Protein Crystallography*, **31,** 34–38
24. Vagin, A., and Teplyakov, A. (1997) *J. Appl. Crystallogr.* **30,** 1022–1025
25. Collaborative Computational Project, Number 4 (1994) *Acta Crystallogr. Sect. D* **50,** 760–763
26. Jones, T. A., Zou, J. -Y., Cowan, S. W., and Kjeldgaard, M. (1991) *Acta Crystallogr. Sect. A* **47,** 110–119
27. Murshudov, G. N., Vagin, A. A., and Dodson, E. J. (1997) *Acta Crystallogr. Sect. D* **53,** 240–255
28. Laskowski, R. A., MacArthur, M. W., Moss, D. S., and Thornton, J. M. (1993) *J. Appl. Crystallogr.* **26,** 283–291
29. Tsodikov, O, V., Record, M. T., Jr., and Sergeev, Y. V. (2002) *J. Comput. Chem.* **23,** 600–609
30. Tettelin, H., Nelson, K. E., Paulsen, I. T., Eisen, J. A., Read, T. D., Peterson, S., Heidelberg, J., DeBoy, R. T., Haft, D. H., Dodson, R. J., Durkin, A. S., Gwinn, M., Kolonay, J. F., Nelson, W. C., Peterson, J. D., Umayam, L. A., White, O., Salzberg, S. L., Lewis, M. R., Radune, D., Holtzapple, E., Khouri, H., Wolf, A. M., Utterback, T. R., Hansen, C. L., McDonald, L. A., Feldblyum, T. V., Angiuoli, S., Dickinson, T., Hickey, E. K., Holt, I. E., Loftus, B. J., Yang, F., Smith, H. O., Venter, J. C., Dougherty, B. A., Morrison, D. A., Hollingshead, S. K., and Fraser, C. M. (2001) *Science* **293,** 498–506
31. Holm, L., and Sander, C. (1993) *J. Mol. Biol.* **233,** 123–138
32. Brookfield, D. E., Green, J., Ali, S. T., Machado, R. S., and Guest, J. R. (1991) *FEBS Lett.* **295,** 13–16
33. Wilson, K. P., Shewchuk, L. M., Brennan, R. G., Otsuka, A. J., and Matthews, B. W. (1992) *Proc. Natl. Acad. Sci. U. S. A.* **89,** 9257–9261
34. Quinn, J. (1997) *Methods Enzymol.* **279,** 193–202
35. Fujiwara, K., Okamura-Ikeda, K., and Motokawa, Y. (1996) *J. Biol. Chem.* **271,** 12932–12936
36. Åberg, A., Yaremchuk, A., Tukalo, M., Rasmussen, B., and Cusack, S. (1997) *Biochemistry* **36,** 3084–3094
37. Kabsch, W., and Sander, C. (1983) *Biopolymers* **22,** 2577–2637
38. Thompson, J. D., Higgins, D. G., and Gibson, T. J. (1994) *Nucleic Acids Res.* **22,** 4673–4680
39. Kraulis, P. J. (1991) *J. Appl. Crystallogr.* **24,** 946–950
40. Merritt, E. A., and Bacon, D. J. (1997) *Methods Enzymol.* **277,** 505–524
41. Esnouf, R. M. (1999) *Acta Crystallogr. Sect. D* **55,** 938–940
42. Wallace, A. C., Laskowski, R. A., and Thornton, J. M. (1995) *Protein Eng.* **8,** 127–134

[3] S. Kure, personal communication.
[4] K. Fujiwara, unpublished observation.

**Crystal Structure of Lipoate-Protein Ligase A from *Escherichia coli*:
DETERMINATION OF THE LIPOIC ACID-BINDING SITE**

Kazuko Fujiwara, Sachiko Toma, Kazuko Okamura-Ikeda, Yutaro Motokawa, Atsushi
Nakagawa and Hisaaki Taniguchi

Access the most updated version of this article at doi: 10.1074/jbc.M505010200

Alerts:

- When this article is cited
- When a correction for this article is posted

Click here to choose from all of JBC's e-mail alerts

This article cites 37 references, 12 of which can be accessed free at
http://www.jbc.org/content/280/39/33645.full.html#ref-list-1